Desalination and Water Treatment
www.deswater.com

doi: 10.5004/dwt.2021.26826

217 (2021) 262–271
March

Extraction model to remove antibiotics from aqueous solution by emulsion and Pickering emulsion liquid membrane

Mohammed A. Atiya[a], Ahmed A. Mohammed[b], Maad A. Hussein[b,*]

[a]*Al-Kawarizmi College of Engineering, University of Baghdad, Baghdad, Iraq, email: mohatiya1965@gmail.com*
[b]*Environmental Engineering Department, University of Baghdad, Baghdad, Iraq, emails: altaaimaad@yahoo.com/ m.altaai@coeng.uobaghdad.edu.iq (M.A. Hussein), ahmed.abedm@yahoo.com (A.A. Mohammed)*

Received 14 May 2020; Accepted 18 November 2020

ABSTRACT

The validity of the mathematical model to extract the antibiotics contaminants such as tetracycline (TC) and ciprofloxacin (CIP) through emulsion and Pickering emulsion liquid membrane (ELM and PELM) was studied in this research. In this work, heptane was used as a diluent, TBP as carrier, HCl as the internal phase, and Span80 or Fe_2O_3 modified with oleic acid as a stabilizing agent. The used mathematical model is already available, but it has not yet been tested for the extraction of any antibiotics before. The model results show a very good matching when compared with the obtained experimental data through various process parameters, including homogenizer speed, surfactant or nanoparticles concentration and carrier concentration. The error percentage was less than 2% for TC and CIP by using ELM process and about 1% for both TC and CIP by using PELM process.

Keywords: Emulsion; Pickering emulsion; Liquid membrane; Mathematical model; Breakage

1. Introduction

Emulsion liquid membrane (ELM) is an attractive method to eliminate a wide range of organic and inorganic contaminants. This method can also be used for the recovery of precious contaminants from the aqueous solutions. ELM consists of a three-phase dispersion system known as the external, membrane and internal phases and the presence of surfactant is essential to encapsulate the internal water phase inside the oil membrane phase [1,2]. The new trend of ELM is familiarized as Pickering emulsion liquid membrane (PELM), which includes the use of nanomaterials as a stabilizing agent instead of the traditional surfactants in ELM technique. The use of nanoparticles offers higher emulsion stability (less membrane breakage) and higher extraction capacity [3,4].

Various mathematical modeling of ELM was studied during the past decades that can be classified into two groups, which are facilitated as diffusion mass transfer model and carrier-mediated mass transfer model. Chakraborty et al. [5] studied the application of unsteady state mathematical model developed by Ho et al. [6] for the separation and concentration of Cu(II) and Ni(II), the model used neglects the effects of membrane breakage and the mass transfer resistance at the external phase. By investigating the effect of many parameters, a good arrangement between the experimental and predicted data was reached. Zeng et al. [7] modified a mathematical model that assumed a dynamic equilibrium between the solute (nickel) and carrier (PC88A) concentration at the external interface. According to the optimal conditions, the extraction efficiency of nickel from sulfate media

* Corresponding author.

reached 93% in 10 min. Kargari et al. [8] studied the modeling of ELM for the selective separation of Au(III) from aqueous solution by using LK-80 as a surfactant and MBIK as a carrier. The obtained results from the model shows a good matching between the experimental and predicted data for the extraction of Au^{3+} from aqueous solution containing Fe^{3+}, Cu^{2+}, Au^{3+}, Pt^{4+}, and Pd^{2+}. Liu and Zhang [9] offered a simplified asymptotic cases model when partial differential equations are adapted to ordinary differential equations. However, Huang et al. [10], and Fan et al. [11] establish a closed-form analytical solution model for the carrier-mediated ELM technique. The simple kinetic model was validated for Pb^{2+} ions transport through liquid membrane [12]. Agarwal et al. [13] presented a mathematical model for the batch extraction of crystal violet and methylene blue in single and binary mixture for the first time.

Our present research studied the mathematical modeling of antibiotic tetracycline (TC) and ciprofloxacin (CIP) by ELM for the first time. Also, to the best of our knowledge, the modeling of PELM was explained for the first time in this study. The membrane phase used consisted of heptane as a diluent, tri-n-butylphosphate as a mobile carrier and Span80 as a stabilizing agent for ELM and Fe_2O_3 nanoparticles modified with oleic acid for PELM. HCl was used in the internal phase and 100 ppm initial concentration was maintained for both TC and CIP in the external phase.

2. Chemical and experimental methods

The emulsion phase was prepared as follows: 25 mL of the membrane phase, which consists of appropriate amounts of stabilizing agent and TBP were dissolved in n-heptane and stirred for 20 min to homogenize it. The internal aqueous phase was formulated by taking an appropriate volume of acidic solution in distilled water and adding it dropwise to the membrane solvent, while the system was being homogenized by using high-speed homogenizer. Before preparing the emulsion phase, 250 mL of the external phase was prepared in 400 mL beaker by dissolving a certain amount of TC or CIP in distilled water to produce 100 mg/L initial concentration. The milky white emulsion was then dispersed into the external solution while stirring the system, and the samples were taken at a certain operation times. All the samples were filtrated using filter syringe of 0.22 μm. Summary of chemicals and the experimental condition were illustrated in Table 1.

3. Theory of the model

The mathematical model developed by Ho and Sirkar [14], which is based on the total mass transfer coefficients and membrane breakage is applied in this study to examine the model validity with the experimental work. The model with a single-solute transport assumes a spherical shell approach as shown in Fig. 1. By two mechanisms, the solute can be transported from the internal phase to the external phase, which is known as (a) diffusional transport and (b) breakage. Via only diffusional transport, the solute is transported from the external to internal solution [13]. The rate of mass transfer (j_k) for diffusional transport can be described as follows:

$$j_k = k' A_V \left(V_i + V_m\right)\left(\frac{K_e}{K_i}C_e - C_i\right) = k\left(V_i + V_m\right)\left(\frac{K_e}{K_e}C_e - C_i\right) \quad (1)$$

where k'(m/s) = overall mass transfer coefficient (depends on the emulsion globules mass transfer area in the external phase), A_V (m^2/m^3) = mass transfer area of the external phase per unit volume of emulsion, V_m and V_i (m^3) = membrane and internal phase volume, respectively, k(s^{-1}) = overall mass transfer coefficient (depends on emulsion volume ($V_i + V_m$), C_e and C_i (g/L) = external and internal solute concentrations, respectively, K_e and K_i = solute distribution coefficient at external-membrane interface and internal membrane interface at equilibrium, respectively.

This indicates that the emulsion volume is proportional to the mass transfer area. While the changes in internal phase volume with time, which is defined by means of breakage, can be calculated as follows:

$$-\frac{dV_i}{dt} = \phi V_i \quad (2)$$

where t = extraction time (s) and ϕ = breakage coefficient (s^{-1}). Then the rate of mass transfer because of the breakage is given as follows:

$$j_\phi = \phi V_i C_i \quad (3)$$

The volume of internal phase as a function of time can be obtained by integrating Eq. (2) into Eq. (4), while the breakage coefficient can be calculated from Eqs. (5) and (6):

$$V_i = V_{i0}\exp\left(-\phi t\right) \quad (4)$$

$$\phi = \frac{-\ln\dfrac{V_i}{V_{i0}}}{t} \quad (5)$$

$$V_i = V_{e0}\frac{10^{-\mathrm{pH}_0} - 10^{-\mathrm{pH}}}{10^{-\mathrm{pH}} - C_{\mathrm{H}^+}^{\mathrm{int}}} \quad (6)$$

where V_{i0} and V_{e0} (m^3) = initial internal and external phase volumes, respectively. The membrane breakage leads to decrease in the internal phase volume and on other hand increases the external phase volume (V_e) as follows:

$$V_e = V_0 - V_i = V_0 - V_{i0}\exp\left(-\phi t\right) \quad (7)$$

where

$$V_0 = V_{i0} + V_{e0} \quad (8)$$

The solute (A) transport from external to internal solution by a mechanisms of diffusional transport (associated

Table 1
Chemical sources, properties and ranges used in the experimental investigations

Material	Source	Properties	Range
		Membrane phase	
Span80 used in the case of ELM	Merck KGaA, Darmstadt, Germany	M.W. = 428.6 g/mol; molecular formula = $C_{24}H_{44}O_6$; saponification value = 145–160; water content ≤1%	2%–6% (v/v)
Fe_2O_3 used in the case of PELM	Merck KGaA, Darmstadt, Germany	M.W. = 159.69 g/mol; assay ≥99.0%	0.3%–0.7% (w/v)
TBP	Merck KGaA, Darmstadt, Germany	M.W. = 266.31 g/mol; molecular formula = $C_{12}H_{27}O_4P$; assay ≥98.5%	2%–6% (v/v)
n-Heptane	Thomas beaker, India	M.W. = 100.2 g/mol; molecular formula = $CH_3(CH_2)_5CH_3$; assay ≥99.0% (GC); solubility in water = 0.0003% (20°C)	22 mL
		Internal phase	
HCl	Thomas beaker, India	M.W. = 36.46 g/mol; solubility in water = 67.3 g/100 g water at 30°C	0.25 M in ELM and 0.1 M in PELM
Distilled water	Chemical materials laboratory, University of Baghdad, Iraq	Electrical conductivity = 1 μS and pH = 7.0	20 mL
		External phase	
Tetracycline	State Company for drag industry and medical appliances (SDI, Iraq).	M.W. = 480.9 g/mol; molecular formula = $C_{22}H_{25}ClN_2O_8$; assay = ≥98%; wavelength = 360 nm	100 ppm
Ciprofloxacin	State Company for drug industry and medical appliances (SDI, Iraq).	M.W. = 331.34 g/mol; molecular formula = $C_{17}H_{18}FN_3O_3$; assay = ≥98%; wavelength = 276 nm	100 ppm
HCl, NaOH for adjusting pH	Thomas beaker, India	For NaOH (M.W) = 40 g/mol; solubility in water = very soluble	
		Other parameters	
Homogenizer speed		3,000–19,700 rpm	
Emulsification time		7 min	
Internal to membrane phase volume ratio		1	
External to emulsion phase volume ratio		5/1	
Agitation speed		250 rpm	

with coefficient of mass transfer, k_A), in which it reacts with stripping agent (HCl) and become the solute (B) as presented schematically in Fig. 1. In addition, the transportation of solute (B) from the internal phase towards the external phase may be occurred by both: (a) diffusional mechanisms (associated with coefficient of mass transfer, k_B), and (b) breakage mechanisms (related to ϕ). Thus, the external phase may contain both solutes (A) and (B); however, the internal phase contains only solute (B). The stripping agent escaped outside the internal phase to external phase may change solute (A) to solute (B), and thus, solute (A) can remain in external solution till its consumed by both extraction mechanism and leaking of stripping agent [13].

The following sets of equations describe the equations of transient mass balance for solute (A), solute (B) and internal agent at $0 \le t \le t_1$ [14]:

$$\frac{d\left(V_e C_{eA}\right)}{dt} = k_{A1}\left(V_m + V_i\right)\left(C_{iA} - \frac{K_{eA}}{K_{iA}} C_{eA}\right) - \phi V_i C_{ir} \tag{9}$$

$$\frac{d\left(V_e C_{eB}\right)}{dt} = k_B\left(V_m + V_i\right)\left(C_{iB} - \frac{K_{eB}}{K_{iB}} C_{eB}\right) + \phi V_i C_{iB} - \phi V_i C_{ir} \tag{10}$$

$$\frac{d\left(V_e C_{ir}\right)}{dt} = k_{A1}\left(V_m + V_i\right)\left(C_{iA} - \frac{K_{eA}}{K_{iA}} C_{eA}\right) - \phi V_i C_{ir} \tag{11}$$

In which t_1 (s) = the time for full solute (A) extraction from the feed solution. K_{eA} and K_{eB} = the equilibrium distribution coefficient of solute (A) and solute (B) between external and membrane phases, K_{iA} and K_{iB} = the equilibrium distribution coefficient of solute (A) and solute (B)

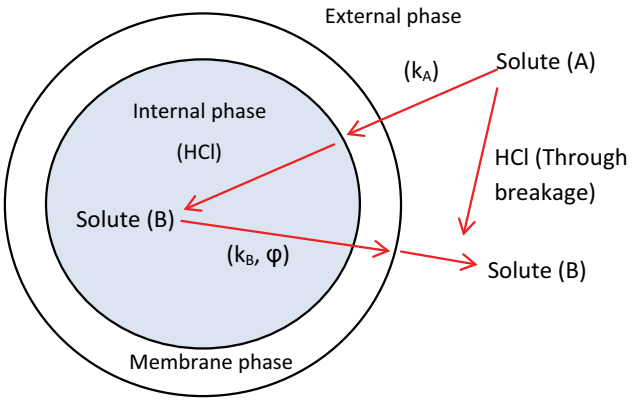

Fig. 1. Schematic of single-solute extraction.

between internal and membrane phases, and r = the internal agent (HCl). By neglecting the accumulation of solute in the organic phase compared with solute amount in internal and external phases, and from the mass conservation equation C_{iB} is given as follows:

$$V_i C_{iB} = C_{eA0} V_{e0} + C_{eB0} V_{e0} + C_{iB0} V_{i0} - C_{eA} V_e - C_{eB} V_e \tag{12}$$

The initial conditions (at t = 0) of Eqs. (7)–(10) are as follows:

$$C_{eA} = C_{eA0}, C_{eB} = C_{eB0}, C_{iB} = C_{iB0}, C_{ir} = C_{ir0}, V_e = V_{e0}, V_i = V_{i0}$$

For the case when solute (B) cannot diffuse across the organic phase (i.e., k_B = 0), and for feasible situation (when k_B = 0, and hence k_B^0), the solute (A) concentration in internal solution (C_{iA}) and solute (B) concentration in the external solution (C_{eB}) are assumed to be zero, then the previous set of equations can be reduced to:

$$\frac{d\left(V_e C_{eA}\right)}{dt} = -k_A^0 C_{eA} - \phi V_i C_{ir} \tag{13}$$

$$\frac{d\left(V_e C_{eB}\right)}{dt} = \phi V_i C_{iB} - \phi V_i C_{ir} \tag{14}$$

$$\frac{d\left(V_e C_{ir}\right)}{dt} = -k_A^0 C_{eA} - \phi V_i C_{ir} \tag{15}$$

$$V_i C_{iB} = C_{eA0} V_{e0} + C_{iB0} V_{i0} - C_{eA} V_e - C_{eB} V_e \tag{16}$$

where C_{eA} and C_{iB} (g/L) = solute (A) concentration in the external phase, and solute (B) concentration in internal phase.

$$k_A^0 = k_A\left(V_i + V_m\right); \quad k_B^0 = k_B\left(V_i + V_m\right) \tag{17}$$

where k_A^0 and k_B^0 (m³/s) = volumetric mass transfer coefficients for solutes (A) and (B), respectively; and supposed to be constant (i.e., emulsion volume or mass transfer area does not change significantly).

k_A and k_B (s^{-1}) = total mass transfer coefficients for solutes (A) and solute (B), respectively. The total mass transfer coefficient is described in Eq. (18) [15]:

$$\frac{1}{K_T} = \frac{1}{K_M} + \frac{1}{K_F} \tag{18}$$

where K_T (m/s) refers to the total mass transfer coefficient and K_M (m/s) represent the mass transfer coefficient for the external phase and is determined from Skell and Lee correlation given in Eq. (19) cited by Raji et al. [16]:

$$\frac{K_M}{\sqrt{ND}} = 2.932 \times 10^{-7}\left(\frac{V_m + V_i}{V_e + V_m + V_i}\right)\left(\frac{d_I}{T}\right)^{0.548} \mathrm{Re}^{1.371} \tag{19}$$

in which N (rpm) signifies the agitated speed of the mixing tank; T and d_I refers to the mixing and impeller tank diameter, respectively; and Re refers to the Reynold number of the continuous phase and is estimated from Eq. (20):

$$R_e = \frac{N d_I^2 \rho_c}{\mu_C} \tag{20}$$

where μ_C and ρ_c are the continuous phase viscosity (kg/ms) and density (kg/m³). Whereas, D is the solute–carrier complex diffusivity in the organic solvent and is calculated from the correlation of Eq. (21) cited by Treybal [17]:

$$D = \frac{\left(117.3 \times 10^{-18}\right)\left(M\phi\right)^{0.5} T}{\mu_m \phi_c^{0.6}} \tag{21}$$

in which M is the solvent molecular weight, ϕ is the solvent association factor, T signifies the temperature in kelvin, μ_m is the viscosity of membrane phase (kg/ms) and ϕ_c is the molar volume of the solute–carrier complex and is estimated by using the Schroeder method [18]. While, K_F (m/s) signifies the interfacial reaction rate constant, and is calculated from Eq. (22):

$$\ln\left(\frac{C_e}{C_{e0}}\right) = -A k_F t \tag{22}$$

where A represent specific interfacial area of the emulsion and is calculated from Eq. (23) [19]:

$$A = \frac{A_i}{V} = \frac{6\alpha}{d_{32}} \tag{23}$$

where A_i is the emulsion droplet interfacial area, V refers to the emulsion unit volume; d_{32} refers to the sauter mean diameter, and α is the water volume fraction.

For typical stability of ELM systems, the membrane breakage can be neglected. Thus, the emulsion volume (i.e., membrane and internal phase volume) does not get affected significantly [13]. The initial conditions for Eqs. (13)–(16), at t = 0 are as follows:

$$C_{eA} = C_{eA0}, \; C_{eB} = C_{eB0}, \; C_{ir} = C_{ir0}, \; V_e = V_{e0}, \; V_i = V_{i0}$$

This model supposed that solute (A) concentration in the feed phase is zero beyond $t = t_1$ (i.e., solute (A)) is eliminated from the feed solution). Then at $t \geq t_1$, the equations of solutes mass balance can be written as follows [14]:

$$C_{eA} = 0 \tag{24}$$

$$\frac{d\left(V_e C_{eB}\right)}{dt} = \phi V_i C_{iB} \tag{25}$$

$$\frac{d\left(V_e C_{ir}\right)}{dt} = -\phi V_i C_{ir} \tag{26}$$

$$V_i C_{iB} = V_{e0} C_{eA0} + V_{i0} C_{iB0} - V_e C_{eB} \tag{27}$$

The following relationship can be obtained by substituting Eq. (13) into Eq. (15) and integrating the resultant equation:

$$V_i C_{ir} = V_{e0} C_{eA0} + V_{i0} C_{ir0} - V_{e0} C_{eA0}, \quad \text{for } 0 \leq t \leq t_1 \tag{28}$$

The set of Eqs. (24)–(27) could be calculated for the two cases of large and small membrane breakage. In this study, a small breakage case was assumed, that is favorable for practical interest of ELM systems. Thus, V_e and V_i is assumed to be constant, and approached to their initial volumes V_{e0} and V_{i0}, respectively. Therefore, solutes (A) and (B) concentration profiles in external phase are solved as follows [14]: For $0 \leq t \leq t_1$,

$$C_{eA} = \frac{\left(k_A^0 C_{eA0} + \phi V_{i0} C_{ir0}\right)}{k_A^0 + \phi V_e} \exp\left(-\left(\phi + \frac{k_A^0}{V_e}\right) t\right) - \phi \frac{\left(V_{i0} C_{ir0} - V_{e0} C_{eA0}\right)}{k_A^0 + \phi V_e} \tag{29}$$

$$C_{eB} = \frac{V_{i0}}{V_e}\left(C_{iB0} + C_{ir0} - \left(C_{iB0} + C_{ir0}\right)\exp\left(-\phi t\right)\right) \tag{30}$$

By assuming $C_{eA} = 0$, t_1 is achieved from Eq. (31):

$$t_1 = \frac{V_e}{k_A^0 + \phi V_e} \ln\left(\frac{k_A^0 C_{eA0} + \phi V_{i0} C_{ir0}}{\phi\left(V_{i0} C_{ir0} - V_{e0} C_{eA0}\right)}\right) \tag{31}$$

At $t \geq t_1$ and $C_{eA} = 0$, the solution of concentration profiles is given below:

$$C_{eB} = \frac{1}{V_e}\left(\begin{array}{l} V_{e0} C_{eA0} + V_{i0} C_{iB0} - V_{i0}\left(C_{iB0} + C_{ir0}\right)\exp\left(-\phi t\right) + \\ \left(V_{i0} C_{ir0} - V_{e0} C_{eA0}\right)\exp\left(-\phi\left(t - t_1\right)\right) \end{array}\right) \tag{32}$$

C_{iB0} is assumed to be zero because the internal phase contains no solute (B) at initial time (i.e., $t = 0$).

Then, the extraction efficiency (%E) of solute (A) is calculated as follows:

$$\%E = \left(1 - \frac{C_{eA} - C_{eB}}{C_{eA0} - C_{eB0}}\right) \times 100 \tag{33}$$

For single-solute transport across the ELM, $C_{eB0} = 0$, Eq. (33) becomes:

$$\%E = \left(1 - \frac{C_{eA} - C_{eB}}{C_{eA0}}\right) \times 100 \tag{34}$$

The sum of errors between the experimental and the predicted data is determined in the following Eq. (35):

$$\%\mathrm{Er} = \sum_i \left(\frac{E_{i,\text{predicted}} - E_{i,\text{experimental}}}{E_{i,\text{experimental}}}\right)^2 \times 100 \tag{35}$$

4. Validity of the mathematical model

The validity of the mathematical model was checked by comparing the obtained experimental data of TC and CIP in both systems of ELM and PELM with the predicted data from the model. The effects of the most important parameters, including homogenizer speed, surfactant or nanoparticles concentration and carrier concentration were studied in this work. The constant parameters k_A^0, ϕ and Er are given in Tables 2 and 3.

4.1. Validity of the ELM system

4.1.1. Effect of homogenizer speed

Homogenizer speed is considered throughout the experimental work to be an important factor in creating a stable emulsion. For TC extraction, Fig. 2 shows a very good matching between the predicted and experimental result. The model also confirms that speed of 12,700 rpm yield in highest extraction efficiency and volumetric mass transfer coefficient of about 88% and 8.74 × 10^{-7} (m^3/s), respectively; as presented in Table 2, which also gives minimum error percentage and breakage coefficient of 2.5% and 1.78 × 10^{-5} (s^{-1}), respectively. However, decreasing the homogenizer speed increasing the error percentage to 9.6%, which means that, at lower speeds, the predicted data will not highly match with the experimental result due to the lower mass transfer coefficients and higher breakage coefficients effects the model calculations, and also lower speeds effect directly the Reynold number.

Fig. 3 shows the extraction behavior of CIP, in which the model has very good match with experimental result and minimum error and breakage coefficient of 1.9% and 0.82 × 10^{-5} (s^{-1}) occurs at homogenizer speed of 12,700 rpm.

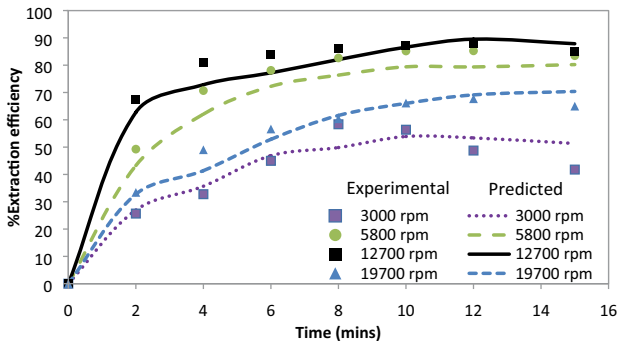

Fig. 2. Variation of TC extraction efficiency with homogenizer speed.

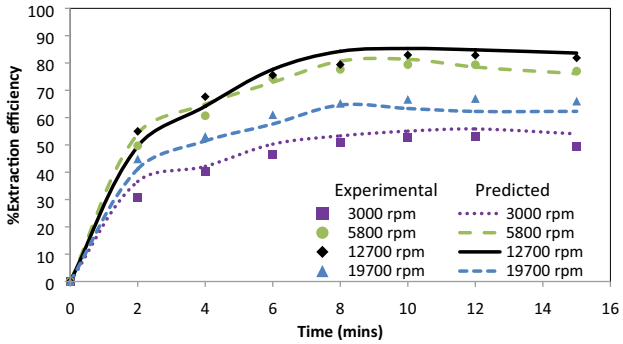

Fig. 3. Variation of CIP extraction efficiency with homogenizer speed.

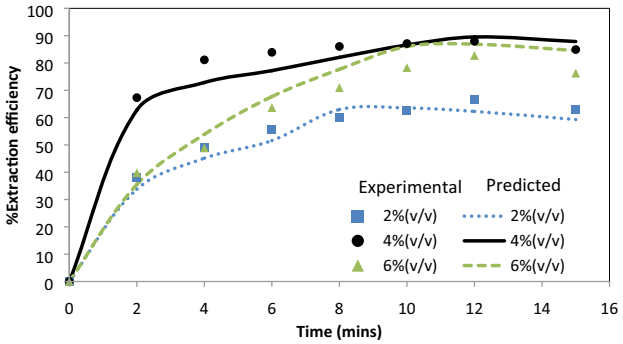

Fig. 4. Variation of TC extraction efficiency with surfactant concentration.

As in TC extraction, the error percentage and breakage coefficients increased to 6.3% and 3.804 × 10^{-5} (s^{-1}), respectively; by decreasing the homogenizer speed, which results in lowest volumetric mass transfer coefficients of 0.54 × 10^{-7} (m^3/s).

4.1.2. Effect of surfactant concentration

Concentration of Span80 was considered in this modeling study due to its significant role in creation of the emulsion phase and the stability and leakage of membrane phase. Figs. 4 and 5 show that modeling of TC and CIP extraction has good matching with the experimental data, and also the model proves that the concentration of 4% yield in the highest extraction percentage for both cases of TC and CIP solutes.

The model parameters in Table 2 reveal that the concentration of 4% (v/v) gives the highest volumetric mass transfer values of 8.74 × 10^{-7} (m^3/s) for TC and 4.36 × 10^{-7} (m^3/s) for CIP compared with 4.21 × 10^{-7} (m^3/s) and 2.51 × 10^{-7} (m^3/s) at concentration of 2% (v/v). This happens due to the presence of more surface acting agent at the emulsion surface, which reduces the breakage coefficient and enhances the mass transfer rate. In addition, concentration of 4% (v/v) yields in lowest error percentage of 2.5% for TC and 1.9% for CIP. Further increase the Span80 concentration to 6%, although the breakage coefficient decreases and the emulsion stability enhances, the extraction efficiency and volumetric mass transfer coefficient decreased to 6.37 × 10^{-7} (m^3/s) and 3.1 × 10^{-7} (m^3/s), for TC and CIP, respectively. This is as a result of the existence of more surfactant at external-membrane interface, which increases the resistance to mass transfer. The same investigation of the effect of surfactant by this model was observed by Agarwal et al. [13].

4.1.3. Effect of carrier concentration

Solute transport process cannot be accomplished without the presence of carrier in the membrane phase; thus TBP concentration was examined by the mathematical model in this study. The variation of extraction efficiency with TBP concentration for TC and CIP are shown in Figs. 6 and 7. The model results presented in the figures proved the experimental investigation, which stated that the best TBP concentration for TC was 4% and for CIP was

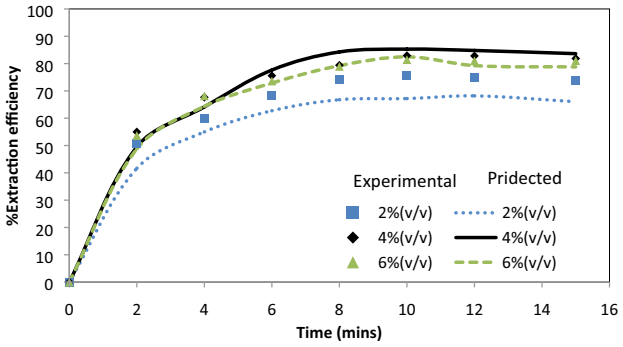

Fig. 5. Variation of CIP extraction efficiency with surfactant concentration.

6%, which provides highest volumetric mass transfer rate of 9.45 × 10^{-7} (m^3/s) for TC and 4.36 × 10^{-7} (m^3/s) for CIP as presented in Table 2. The breakage coefficient (ϕ) increased with increasing the carrier concentration due to competitive reaction and adsorption of the carrier TBP with surface acting agent (Span80) at the emulsion surface lead to more release of the internal constituent. The error percentage between the predicted and experimental result was high at low carrier concentration and decreased with increasing the carrier concentration as shown in Table 2, which mean more matching between the predicted and experimental results.

4.2. Validity of the PELM system

4.2.1. Effect of homogenizer speed

In PELM, homogenizer speed is also considered an important parameter through the experimental work for creating the emulsion. For TC extraction, Fig. 8 shows a good similarity between the results of the predicted and experimental data. The model confirms the experimental results in which the speed of 12,700 rpm yield in maximum extraction efficiency and the volumetric mass transfer coefficient was highest 14.51 × 10^{-7} (m^3/s), as presented in Table 3, which also gives minimum error percentage and breakage coefficient of 4.34% and 4.77 × 10^{-5} (s^{-1}), respectively. Fig. 9 shows the extraction behavior of CIP, in which the model has a very good matching with experimental result and minimum error percentage of 1.9% and breakage coefficient of 0.82 × 10^{-5} (s^{-1}), occurs at homogenizer speed of 12,700 rpm.

Table 2
Model parameters for ELM system

Operating parameters	Value	Tertracycline			Ciproloxacin		
		Φ ($\times 10^5$ s^{-1})	k_A^0 ($\times 10^7$ m^3/s)	%Er	Φ ($\times 10^5$ s^{-1})	k_A^0 ($\times 10^7$ m^3/s)	%Er
Homogenizer speed, rpm	3,000	31.1	1.22	9.67	38	0.54	6.32
	5,800	8.66	4.17	5.21	6.81	1.87	1.53
	12,700	1.78	8.74	2.51	3.37	4.36	1.9
	19,700	1.32	3.79	3.69	4.26	1.36	2.17
Surfactant concentration, %v/v	2	4.03	4.21	3.46	8.62	2.51	8.69
	4	1.78	8.74	2.51	3.37	4.36	1.9
	6	1.32	6.73	5.86	3.37	3.10	1.3
TBP concentration, %v/v	2	0.881	2.43	9.66	0.528	0.81	14
	4	0.881	9.45	1.67	0.824	2.31	1.17
	6	3.59	6.52	0.38	0.824	4.36	1.51

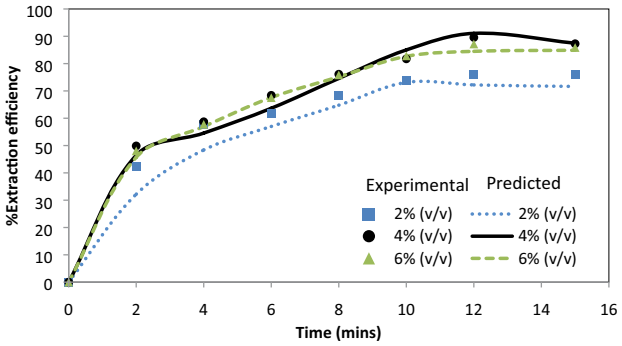

Fig. 6. Variation of TC extraction efficiency with TBP concentration.

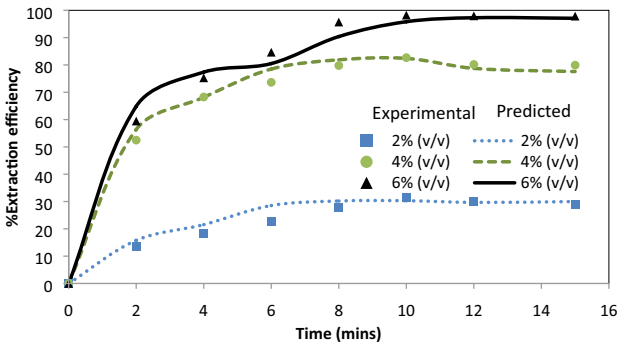

Fig. 7. Variation of CIP extraction efficiency with TBP concentration.

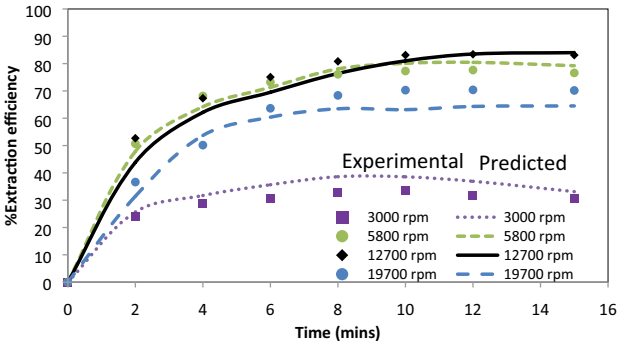

Fig. 8. Variation of TC extraction efficiency with homogenizer speed.

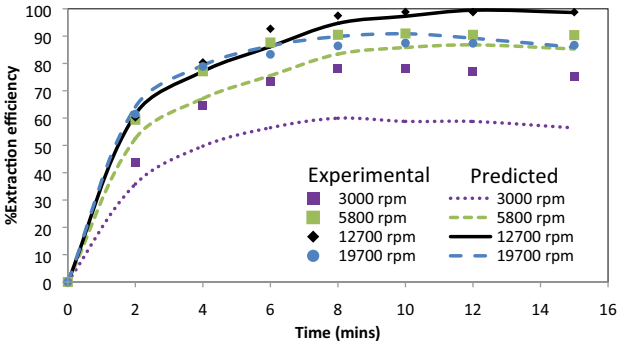

Fig. 9. Variation of CIP extraction efficiency with homogenizer speed.

However, lowering the speeds result in higher error percentage and the predicted data will be far away from the experimental investigations. The error percentage increased to 12.7% and 37.6% for TC and CIP, respectively; at homogenizer speed of 3,000 rpm. This is because of the lower volumetric mass transfer coefficients and higher breakage coefficients (23.4×10^{-5} (s^{-1}) for TC and 13.9×10^{-5} (s^{-1}) for CIP) effects on model calculations, and also lower speeds effect directly on the Reynold number.

4.2.2. Effect of nanoparticles concentration

Fe_2O_3 nanoparticles were incorporated in the membrane phase instead of surfactant as a stabilizing agent, and it was considered in this study due to its significant role in creation and stability of the emulsion phase. Figs. 10 and 11 show that modeling data of TC and CIP extraction have good matching with their experimental data, and also the model proves that the concentration of 0.7% yield in the

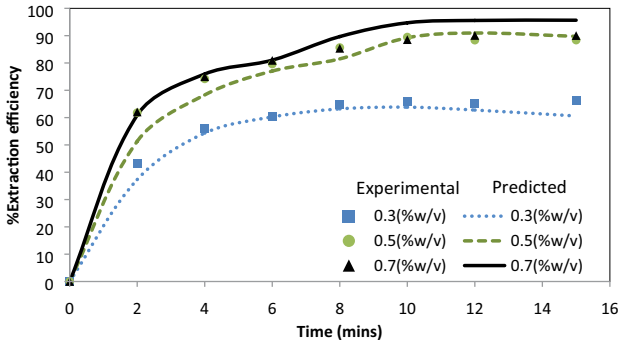

Fig. 10. Variation of TC extraction efficiency with Fe_2O_3 concentration.

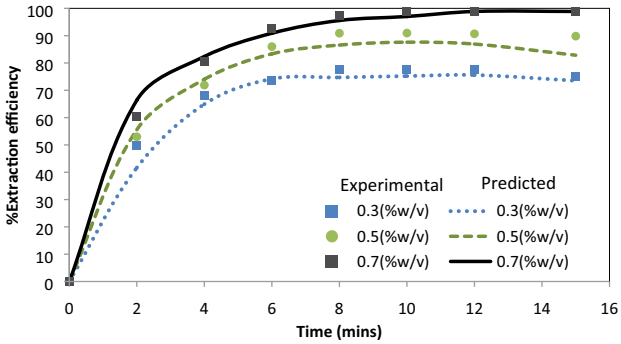

Fig. 11. Variation of CIP extraction efficiency with Fe_2O_3 concentration.

Table 3
Model parameters for PELM system

Operating parameters	Value	Tertracycline			Ciprofloxacin		
		Φ ($\times 10^5$ s^{-1})	k_A^0 ($\times 10^7$ m^3/s)	%Er	Φ ($\times 10^5$ s^{-1})	k_A^0 ($\times 10^7$ m^3/s)	%Er
Homogenizer speed, rpm	3,000	23.45	2.37	12.7	13.9	0.309	37.6
	5,800	6.28	8.39	1.16	4.25	2.25	6.34
	12,700	4.77	14.51	4.34	0.105	9.204	1.2
	19,700	10.68	7.64	5.71	3.37	1.607	1
Fe_2O_3 concentration, %w/v	0.3	13.8	1.37	2.91	8.62	2.062	3.16
	0.5	3.59	7.49	3.95	1.34	3.814	1.55
	0.7	1.92	14.51	1.55	0.105	9.204	1.2
TBP concentration, %v/v	2	0.572	3.09	9.4	0.007	1.034	11.4
	4	0.572	11.72	1.77	0.105	3.675	3.6
	6	1.29	13.33	4.9	0.105	9.204	1.2

highest extraction percentage and membrane stability and lowest error percentage of 1.5% for TC and 1.2% for CIP.

The model parameters shown in Table 3 reveals that the concentration of 0.7% gives the highest volumetric mass transfer values of 14.5 × 10^{-7} (m^3/s) for TC and 9.2 × 10^{-7} (m^3/s) for CIP compared with 1.37 × 10^{-7} (m^3/s) and 2.06 × 10^{-7} (m^3/s) at concentration of 0.3%, respectively. This is because of the presence of more nanoparticles at the internal membrane interface, which reduces the breakage coefficient (1.92 × 10^{-5} (s^{-1}) for TC and 0.1 × 10^{-5} (s^{-1}) for CIP) and enhances the mass transfer rate.

4.2.3. Effect of carrier concentration

The existence of the capture agent in the membrane phase is necessary to complete the extraction process. TBP concentration was examined by the mathematical model in this study and the variation of extraction efficiency with TBP concentration for TC and CIP are shown in Figs. 12 and 13. The model results presented in these figures proved the experimental investigation, which stated that the optimum TBP concentration for TC was 4% and for CIP was 6%, that provides highest volumetric mass transfer rate of 11.72 × 10^{-7} (m^3/s) for TC and 9.204 × 10^{-7} (m^3/s) for CIP as presented in Table 3. The breakage coefficients (ϕ)

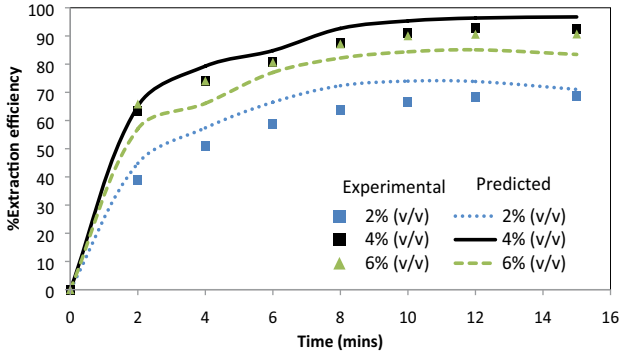

Fig. 12. Variation of TC extraction efficiency with TBP concentration.

were not highly affected at various carrier concentrations and it tends to increase slightly with increasing TBP concentration, which may be due to the competitive adsorption of the carrier material with the nanoparticles. The error percentage increased at low concentration due to the less carrier material affects the diffusion coefficient and the creation of solute–carrier complex, which has direct effect on the mass transfer coefficients and the model calculations.

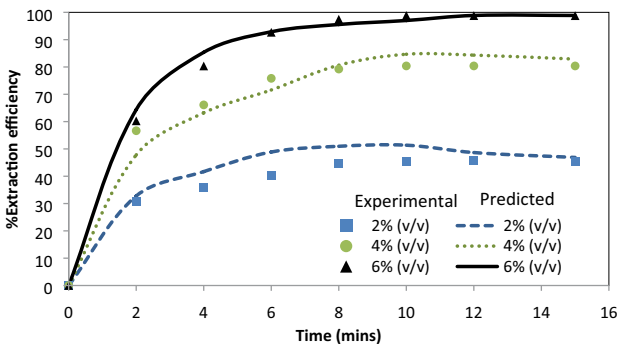

Fig. 13. Variation of CIP extraction efficiency with TBP concentration.

5. Conclusion

The mathematical model successfully used to predict the extraction efficiency of both antibiotics TC and CIP by ELM and PELM systems. The model also shows a very good matching with the experimental investigation through various process parameters. In which the error percentage was less than 2% for TC and CIP by ELM process, and about 1% for TC and CIP by PELM process. The applying of the mathematical model did not show a difference between using ELM or PELM process, in which the use of nanoparticles does not have significant effect on the prediction of the model. However, it only affected the breakage coefficient.

Symbols

A_v — External phase mass transfer area per unit volume of the emulsion, m^{-1}
C_e — Solute concentration in the external phase, g/L
C_{e0} — Initial solute concentration in the external phase, g/L
C_{eA} — Solute (A) concentration in the external phase, g/L
C_{eA0} — Initial solute (A) concentration in the external phase (g/L), g/L
C_{eB} — Solute (B) concentration in the external phase, g/L
C_{eB0} — Initial solute (B) concentration in the external phase, g/L
C_i — Solute concentration in the internal phase, g/L
C_{iB} — Solute (B) concentration in the internal phase, g/L
C_{iB0} — Initial solute (B) concentration in the internal phase, g/L
C_{ir} — Concentration of the reagent in the internal phase, g/L
C_{ir0} — Initial concentration of the reagent in the internal phase, kg/m^3
$E_{i,\text{predicted}}$ — Predicted extraction efficiency, %
$E_{i,\text{experimental}}$ — Experimental extraction efficiency, %
k — Overall mass transfer coefficient, s^{-1}
k_A^0 — $k_A(V_m + V_i)$, m^3/s
k_B^0 — $k_B(V_m + V_i)$, m^3/s
k_A — Overall mass transfer coefficient for solute (A), s^{-1}
k_{A1} — $k_A K_{iA}/K_{eA}$, s^{-1}
k_B — Overall mass transfer coefficient for solute (B), s^{-1}
K_e — Distribution coefficient for the solute between the membrane and external phases at equilibrium
K_{eA} — Distribution coefficient for solute A between the membrane and external phases at equilibrium
K_{eB} — Distribution coefficient for solute B between the membrane and external phases at equilibrium
K_i — Distribution coefficient for the solute between the membrane and internal phases at equilibrium
K_{iB} — Distribution coefficient for solute B between the membrane and internal phases at equilibrium
V_0 — $(V_{e0} + V_{i0}) = (V_e + V_i)$, m^3
V_{e0} — Initial volume of the external phase, m^3
V_{i0} — Initial total volume of the internal phase, m^3
Φ — Breakage coefficient, s^{-1}

References

[1] M.A. Hussein, A.A. Mohammed, M.A. Atiya, Application of emulsion and Pickering emulsion liquid membrane technique for wastewater treatment: an overview, Environ. Sci. Pollut. Res., 26 (2019) 36184–36204.
[2] A.A. Mohammed, M.A. Atiya, M.A. Hussein, Simultaneous studies of emulsion stability and extraction capacity for the removal of tetracycline from aqueous solution by liquid surfactant membrane, Chem. Eng. Res. Des., 159 (2020) 225–235.
[3] A.A. Mohammed, M.A. Atiya, M.A. Hussein, Studies on membrane stability and extraction of ciprofloxacin from aqueous solution using Pickering emulsion liquid membrane stabilized by magnetic nano-Fe_2O_3, Colloids Surf., A, 585 (2020) 124044, https://doi.org/10.1016/j.colsurfa.2019.124044.
[4] A.A. Mohammed, M.A. Atiya, M.A. Hussein, Removal of antibiotic tetracycline using nano-fluid emulsion liquid membrane: breakage, extraction and stripping studies, Colloids Surf., A, 595 (2020) 124680, https://doi.org/10.1016/j.colsurfa.2020.124680.
[5] M. Chakraborty, C. Bhattacharya, S. Datta, Mathematical modeling of simultaneous copper(II) and nickel(II) extraction from wastewater by emulsion liquid membranes, Sep. Sci. Technol., 38 (2003) 2081–2106.
[6] W.S. Ho, T.A. Hatton, E.N. Lightfoot, N.N. Li, Batch extraction with liquid surfactant membranes: a diffusion controlled model, AIChE J., 28 (1982) 662–670.
[7] L.L. Zeng, W.Y. Wang, W. Chen, C. Bukirwa, Y.Q. Yang, Experimental and modeling of nickel removal from sulfate solutions by emulsion liquid membrane using PC 88A, Desal. Water Treat., 57 (2016) 11184–11194.
[8] A. Kargari, T. Kaghazchi, B. Mardangahi, M. Soleimani, Experimental and modeling of selective separation of gold(III) ions from aqueous solutions by emulsion liquid membrane system, J. Membr. Sci., 279 (2006) 389–393.
[9] X.R. Liu, X.J. Zhang, Simplified model for extraction of rare-earth ions using emulsion liquid membrane, J. Membr. Sci., 128 (1997) 223–229.
[10] C.-R. Huang, H.F. Fan, D.W. Zhou, A closed-form solution for a mathematical model of emulsion liquid membrane, J. Membr. Sci., 339 (2009) 233–238.

[11] H.F. Fan, H.Y. Zhang, H. Xie, S.L. Qu, Singularity in a mathematical model of emulsion liquid membrane, Appl. Math. Modell., 36 (2012) 3736–3742.
[12] A.D. Albdiri, A.A. Mohammed, M. Hussein, S.J.D. Koter, Modeling of lead ions transport through a bulk liquid membrane, Desal. Water Treat., 181 (2020) 213–220.
[13] A.K. Agarwal, C. Das, S. De, Modeling of extraction of dyes and their mixtures from aqueous solution using emulsion liquid membrane, J. Membr. Sci., 360 (2010) 190–201.
[14] W. Ho, K. Sirkar, Membrane Handbook, Springer Science & Business Media, 2012.
[15] H. Kasaini, F. Nakashio, M. Goto, Application of emulsion liquid membranes to recover cobalt ions from a dual-component sulphate solution containing nickel ions, J. Membr. Sci., 146 (1998) 159–168.
[16] M. Raji, H. Abolghasemi, J. Safdari, A. Kargari, Response surface optimization of dysprosium extraction using an emulsion liquid membrane integrated with multi-walled carbon nanotubes, Chem. Eng. Technol., 41 (2018) 1857–1870.
[17] R.E. Treybal, Mass – Transfer Operations, 3rd ed., McGraw-Hill Book Co., Singapore, 1981.
[18] B.E. Poling, J.M. Prausnitz, J.P. O'connell, The Properties of Gases and Liquids, McGraw-Hill, New York, 2001.
[19] V. Karcher, F.A. Perrechil, A.C. Bannwart, Interfacial energy during the emulsification of water-in-heavy crude oil emulsions, Braz. J. Chem. Eng., 32 (2015) 127–137.